New insights into the specificity and processivity of two novel pectinases from Verticillium dahliae

Josip Safran, Olivier Habrylo, Mehdi Cherkaoui, Sylvain Lecomte, Aline Voxeur, Serge Pilard, Solène Bassard, Corinne Pau-Roblot, Davide Mercadante, Jérôme Pelloux, et al.

New insights into the specificity and processivity of two novel pectinases from *Verticillium dahliae*

AUTHORS LIST

Josip Safran[a], **Olivier Habrylo**[a], **Mehdi Cherkaoui**[a], **Sylvain Lecomte**[b], **Aline Voxeur**[c], **Serge Pilard**[d], **Solène Bassard**[a], **Corinne Pau-Roblot**[a], **Davide Mercadante**[e], **Jérôme Pelloux**[a], **Fabien Sénéchal**[a,*]

[a]: UMRT INRAE 1158 BioEcoAgro – BIOPI Biologie des Plantes et Innovation, SFR Condorcet FR CNRS 3417, Université de Picardie, 33 Rue St Leu, 80039 Amiens, France. [b]: Linéa Semences, 20 Avenue Saget, 60210 Grandvilliers, France. [c]: Institut Jean-Pierre Bourgin, INRAE, AgroParisTech, Université Paris-Saclay, 78000 Versailles, France. [d]: Plateforme Analytique, Université de Picardie, 33 Rue St Leu, 80039 Amiens, France. [e]: School of Chemical Sciences, The University of Auckland, Private Bag 92019, Auckland 1142, New Zealand.

* Corresponding author

Abstract

Pectin, the major non-cellulosic component of primary cell wall can be degraded by polygalacturonases (PGs) and pectin methylesterases (PMEs) during pathogen attack on plants. We characterized two novel enzymes, VdPG2 and VdPME1, from the fungal plant pathogen *Verticillium dahliae*. VdPME1 was most active on citrus methylesterified pectin (55-70 %) at pH 6 and a temperature of 40 °C, while VdPG2 was most active on polygalacturonic acid at pH 5 and a temperature of 50 °C. Using LC-MS/MS oligoprofiling, and various pectins, the mode of action of VdPME1 and VdPG2 were determined. VdPME1 was shown to be processive, in accordance with the electrostatic potential of the enzyme. VdPG2 was identified as endo-PG releasing both methylesterified and non-methylesterified oligogalacturonides (OGs). Additionally, when flax roots were used as substrate, acetylated OGs were detected. The comparisons of OGs released from *Verticillium*-susceptible and partially resistant flax cultivars identified new possible elicitor of plant defence responses.

Keywords: Pectin**,** polygalacturonase, pectin methylesterase, flax, oligogalacturonides, *Verticillium dahliae*

1. Introduction

The plant cell wall is a complex and dynamic structure of proteins and polysaccharides, consisting of a hydrogen-bonded network of cellulose microfibrils and hemicelluloses embedded in a matrix of pectins [1]. Pectins are the most complex combination of plant cell wall polysaccharides and are found in the middle lamella and primary cell walls of dicotyledonous plants, where they can contribute up to 30 % of dry cell mass [2]. The composition of pectin differs depending on plant species and organs, but generally consist mainly of homogalacturonan (HG), rhamnogalacturonan I (RG-I) and rhamnogalacturonan II (RG-II) domains. HG, which is a linear homopolymer of α-1,4-linked galacturonic acids (GalA), is the most abundant pectic domain representing up to 65 % of pectin [3]. HG can be methylesterified at the C-6 carboxyl and can be O-acetylated at O-2 or O-3. HG chains can be modified by different enzyme families, including pectin acetylesterase (PAEs; EC 3.1.1.6), pectin methylesterases (PMEs; CE8, EC 3.1.1.11), polygalacturonases (PGs; GH28, EC 3.2.1.15*,* EC 3.2.1.67, EC 3.2.1.82), pectate lyases (PLs; EC 4.2.2.2) and pectin lyase (PNLs, EC 4.2.2.10). While these enzymes are endogenously produced by plants to fine-tune pectin structure during development, they are also secreted by some bacteria, fungi, insects and nematodes during plant infestation [4–8]. PMEs act on methylesterified GalA chain where they hydrolyse the O6-ester linkage between methyl group and GalA. PAE play similar role by hydrolysing the O2-acetylated linkage. Demethylesterification makes HG more susceptible to degradation by pectin-degrading enzymes such as PLs, PNLs and PGs [9]. PMEs may differ with respect to their pH optimum, substrate specificity and salt requirements, and have an optimum activity between pH 4-6 for fungal PMEs and pH 6-8 for plant PMEs [10]. It has been shown that plant and bacterial PMEs remove long stretches of methyl groups in a processive manner before dissociating from the HG chain, whereas fungal enzymes act more randomly and are considered as non-processive PMEs [11]. PGs are a family of hydrolases that cut the HG chain releasing oligogalacturonides (OGs) of different degree of polymerisation (DP) and methylesterification/acetylation. Depending on their mode of action, PGs are subdivided into endo-PGs (EC 3.2.1.15), which randomly hydrolyse internal sites and exo- PGs (EC 3.2.1.67, EC 3.2.1.82) that hydrolyse HG from non-reducing end, creating monomers or dimers of GalA. These two types of PGs preferably act on

partially demethylesterified HG chains and have been identified in various fungal species where they can be a determinant of the pathogenicity [12]. Indeed, various fungi secrete pectinases, including PGs to degrade plant cell walls, and invade cells. For instance, it has been shown that Botrytis PG1 and Verticillium PG1 are important virulence factors in tomato and cotton [13,14]respectively. *Verticillium dahlia*e Kleb soil-borne vascular fungus, which attack a broad range plants and has increasing effects on flax species, also produces a number of pectinases for degrading cell wall. Infection of *V.dahliae* occurs at the root surface levels, later invading xylem vessels with progression in acropetal direction [15,16]. To date, without effective chemical control, there is no flax cultivar totally resistant to Verticillium wilt [16], thus it appears of prime importance to understand the pathogenicity of this fungus by characterizing pectinases such as PGs and PMEs. Such a characterisation is indeed required to devise strategies useful to control or inhibit pathogenic activity and must occur on multiple levels: from the characterisation of the protein mechanism of action to the enzymatic structures and dynamics, which provide information on substrate specificity and processive tendencies of different PMEs and PGs. Considering the large number of protein isoforms and ubiquitous presence of PMEs and PGs across plants, bacterial and fungi, relating the functional behaviour and the structural features of PGs and PMEs is challenging. The lack of knowledge for these enzymes is aggravated by the relatively scarce number of resolved structures, compared to the whole number of PGs and PMEs isoforms. More recently the *in-silico* comparison of PMEs electrostatic potentials has underscored the relation between protein electrostatics and substrate specificity, highlighting the importance of balancing electrostatic vs. hydrophobic interactions within the binding groove of PMEs to promote fine-tuning of substrates specificity and different processivity profiles [17]. Although the fold of PGs and PMEs is conserved, with a binding groove able to allocate approximately 10 saccharide units [18] in as many subsites, subtle differences exist between the chemical microenvironments of different subsites, which can either bind, with different affinities, negatively charged, carboxy-methylated or O-acetylated saccharide units. The structural and biochemical description of newly identified PGs and PMEs, with the combination of *in-vitro, ex-vivo* and *in-silico* methods, thus become powerful tools to characterize and contextualize the action of these enzymes within plant physiology and pathology.

The aims of this study are to characterize two novel enzymes from *V. dahliae*, VdPME1 (VDAG_05799) and VdPG2 (VDAG_04977) using biochemical and computational approaches. In particular, their mode of action can determined using a recently developed SEC-MS technique [19], which enables analysis of the OGs generated from commercial pectin as well from flax roots. Our hypothesis is that we can relate the structure of enzymes to their processivity and this can have impact on the OG produced during plant-pathogen interactions.

2. Material and methods

2.1. Bioinformatical analysis

V. dahliae PGs and PMEs were identified using publicly available genome data (ftp.broadinstitute.org/). Sequences were checked for signal peptide using SignalP-5.0 Server (http://www.cbs.dtu.dk/services/SignalP/). Glycosylation sites were predicted using NetNGlyc 1.0 Server (http://www.cbs.dtu.dk/services/NetNGlyc/) and NetOGlyc 4.0 Server (http://www.cbs.dtu.dk/services/NetOGlyc/). The sequence alignments were performed using MEGA multiple sequence alignment program. UCSF Chimera (http://www.cgl.ucsf.edu/chimera/) was used for creation of graphics.

2.2. Modelling, calculations and comparison of protein electrostatic

VdPME1 and VdPG2 models were created using I-TASSER structure prediction software (https://zhanglab.ccmb.med.umich.edu/I-TASSER/). The linearized version of the Poisson-Boltzmann equation was used to solve the electrostatic potentials of the PMEs from *Verticillium dahliae*, *Dickeya chrysanthemi, Citrus sinensis* and *Daucus carota* after that radii and partial charges were assigned to each atom of the structures according to the parameters from the AMBER99 force field [20]by using PDB2PQR (version 2.1.1, [21]).

The PMEs structures were superimposed to fairly compare the electrostatic potential differences across the calculated grids, and the electrostatic potentials were calculated using the APBS software version 3 [22]. The potentials were computed at pH 7, which is the pH used for the activity tests of VdPME1, with protonation states of single residues assigned using the PROPKA software, version 3.3 [23]. Poisson-Boltzmann equation was solved by discretizing the molecule on a 19.3 nm^3 grid (grid spacing equal to $6x10^{-2}$ nm) centred on the C_α atom of one of the PMEs catalytic aspartic acid residues, conserved across PMEs. The computation of the electrostatic

potential was carried out considering a dielectric term of 78.5 for the solvent, in order to account for an aqueous environment, with solute dielectric set to 4.0 and temperature set at 298.15 K.

Electrostatic potentials were numerically compared by calculating electrostatic similarity indices [24,25]. We calculated the cross-product between two electrostatic potentials calculated at each grid point as follows:

$$SI_{a,b}^{H} = \frac{2\phi_a(i,j,k)\phi_b(i,j,k)}{\left(\phi_a^2(i,j,k) + \phi_b^2(i,j,k)\right)}$$

Where $\phi_a^2(i,j,k)$ and $\phi_b^2(i,j,k)$ are the electrostatic potentials calculated at the grid points *i,j,k* for proteins *a* and *b* [24,25].

2.3. Fungal strain and growth

V.dahliae was isolated from CALIRA company flax test fields (Martainneville, France) and was kindly provided by Linéa-Semences company (Grandvilliers, France). Fungus was grown in flasks containing 50 mL M3 medium [26] enriched with different carbon source: polygalacturonic acid sodium salt (PGA, P3850, Sigma) and pectin esterified potassium salt from citrus fruit (55-70 % methylesterified, P9436, Sigma) at 10 $g.L^{-1}$ in order to stimulate *PG* and *PME* expression and secretion. Flasks were kept 15 days in dark condition under 25°C, 80 rpm agitation, and mycelium was harvested by vacuum filtration using Buchner flask. Fresh mycelium was frozen in liquid nitrogen, lyophilized and ground using mortar and pestle. Total RNA isolation cDNA synthesis was as previously described in Lemaire et al. 2020 [27].

2.4. Cloning and heterologous expression of VdPG2 and VdPME1

One PG, VDAG_04977 (hereafter named VdPG2, gene ID: 20706440) and one PME, VDAG_05799 (hereafter named VdPME1, gene ID: 20707262) were amplified using cDNA and gene-specific primers listed in **Table 1** excluding the signal peptide.

Table 1. Primers used for cloning *Verticillium dahliae* enzymes into pPICzαB expression vectors. VdPG2: Polygalacturonase; VdPME1: Pectin methylesterase. Restriction enzymes sites for *Eco*RI, *Pst*I, *Not*I are underlined, added bases are written in *italics*.

Enzyme	Gene ID	Forward 5'- 3'	Reverse 3'- 5'
VdPG2	20706440	*TCTAA*GAATTC*AC*AACCCTCTTCCCGCCAAG	*TGCAC*GCGGCCGCAGAGCACGCGGCAGGG
VdPME1	20707262	*TCTAA*CTGCAG*GA*GCCACGAGGACCTCG	*TGCAC*GCGGCCGCCATGTACGAAGCGTCATAGTAG

Amplified genes were gel purified with gel extraction kit (Neo biotech, Nanterre, France), ligated to pPICZαB (Invitrogen, Carlsbad, California, United States) in frame with His-tag, previously digested with *Pst*1 and *Not*1 for VdPG2 and *Eco*R1 and *Not*1 for VdPME1, and used for transformation of *E. coli* TOP10 (Invitrogen). After sequencing, linearized vector was used to transform *Pichia pastoris* X33 strain as described in the instruction manual EasySelect Pichia Expression Kit manual (Invitrogen).

2.5. VdPG2 and VdPME1 expression, purification and enzyme analysis

VdPG2 and VdPME1 were produced in *Pichia pastoris* as described in the EasySelect Pichia Expression Kit manual (Invitrogen) and in Lemaire et al. (2020). After purification, enzyme buffer was changed to reaction buffer using PD Spintrap G-25 column (GE Healthcare). Determination of protein concentration, glycosylation patterns, enzyme purity and molecular weight were as described in Lemaire et al. 2020 [27].

2.6. VdPG2 and VdPME1 biochemical characterization

The substrate specificity of VdPG2 was determined with the DNS method [28] using polygalacturonic acid (81325, Sigma); Citrus pectin with degree of methylesterification (DM) 20-34 % (P9311, Sigma), DM 55-70 % (P9436, Sigma) or DM >85 % (P9561, Sigma); apple pectin with DM 70-75 % (76282, Sigma); sugar

beet pectin with DM 42 % and degree of acetylation 31 % (DA, CP Kelco, Atlanta, United States) using $2.45.10^{-3}$ µg.µL^{-1} VdPG2 as described in Habrylo et al. 2018 [4]. Results were expressed as nmol of GalA.min^{-1}.µg^{-1} of proteins.

The substrate specificity of VdPME1 was determined using above-mentioned substrates and the alcohol oxidase assay [29,30] with modifications as described in L'Enfantet al. 2019 [31]). VdPME1 concentration was $2.3.10^{-3}$ µg.µL^{-1}. Results were expressed as nmol of MeOH.min^{-1}.µg^{-1} of proteins.

2.7. VdPG2 and VdPME1 temperature, salt and pH dependency assay

The VdPG2 optimum temperature was determined by incubating the enzymatic reaction from 20 to 70 °C during 60 min using polygalacturonic acid (0.4 %, w/v) diluted in 50 mM ammonium acetate buffer (pH 5). The VdPG2 pH optimum was determined between pH 3 and 8 using sodium acetate buffer (pH 3 to 5) and Tris-HCl buffer (pH 6 to 8) and PGA as a substrate at 0.4 % (w/v) final concentration. The VdPME1 pH optimum was determined by mixing citrus pectin DM 55-70 % (P9436, Sigma) at 0.4 % (w/v) final concentration using sodium acetate buffer (pH 3 to 5) and Tris-HCl buffer (pH 6 to 9). The VdPME1 optimum temperature was determined by incubating the enzymatic reaction from 10 to 60 °C using citrus pectin DM 55-70 % (P9436, Sigma) at 0.4 % (w/v) diluted in 50 mM sodium phosphate buffer (pH 7) as mentioned above. VdPME1 activity was calculated using a standard curve between saponified and non-saponified samples as nmol of MeOH.min^{-1}.µg^{-1} of proteins. All experiments were conducted in triplicate.

2.8. Determination of Km, Vmax, and specific activity

The VdPG2 kinetic parameters were calculated using GraFit7 software (Michaelis-Menten/Hill; Erithacus Software, Horley, Surrey, UK) using PGA as a substrate. The reactions were performed using 1 to 20 mg. mL^{-1} PGA concentrations at 50 mM sodium acetate (pH 5) during 10 min at 50 °C. The same procedure was used for VdPME1 with 1 to 20 mg. mL^{-1} pectin DM 55-70 % concentrations in 50 mM sodium phosphate buffer (pH 7) during 20 min at 30 °C.

2.9. Oligoprofiling of digested commercial pectins

Oligogalacturonides (OGs) released after digestions by recombinant VdPG2 and VdPME1 were identified as described in Voxeur et al. 2019 [19]. Briefly, citrus pectin

of DM 24-30 % (P9311, P9436, Sigma), DM 55-70 % (P9436, Sigma) or DM >85 % (P9561, Sigma) were prepared at 0.4 % (w/v) final concentration in 50 mM ammonium acetate buffer (pH 5) and incubated with VdPG2 at $2.45.10^{-3}$ $\mu g.\mu L^{-1}$ concentration during 15 min, 45 min, 90 min, 180 min and overnight at 40 °C. To analyse the processivity of VdPME1, citrus pectins DM 55-70 % (P9436, Sigma) were digested with VdPG2 for 2 h (to obtain OG of various DP and DM) as mentioned above. Resulting OGs were lyophilised, and resuspended in 90 µL 50 mM Tris-HCl buffer (pH 7). 10 µL of VdPME1 at $2.3.10^{-3}$ $\mu g.\mu L^{-1}$ concentration was added and the reaction was incubated for 15 min and overnight at 40 °C. The rest of the procedure was as previously described. Pellets were resuspended in 200 µL dH_2O.

2.10.Oligoprofiling of digested cell wall pectins from flax roots

Flax seeds from two different cultivars, Évéa (partially resistant to *Verticillium* wilt) and Violin (more susceptible to *Verticillium* wilt) were kindly provided by Linéa-Semences (Grandvilliers, France). Seeds were sterilized using Triton 0.01 % (w/v, T8787, Sigma) diluted in ethanol 70 % (w/v) and dried overnight. Seeds grew during three days on wet towel tissue at 21 °C, 16 h/8 h light/dark. Forty roots were cut and placed into ethanol 100 % (w/v) for 24 h. They were washed two times for 5 min with acetone 100 % (w/v) and left to dry 24 h. Roots were rehydrated in 140 µL 50 mM ammonium acetate pH 5 during 2 h at room temperature and digested with VdPG2 at $2.45.10^{-3}$ $\mu g.\mu L^{-1}$ concentration, using the above-mentioned protocol.

2.11.Ultra-performance size-exclusion chromatography (UP-SEC) coupled with electrospray ionization high-resolution mass spectrometry (ESI-HRMS)

OGs produced from above-mentioned commercial pectins and flax roots after digestion were subjected to chromatographic separations and MS-detection as described in Hocq et al. 2020 [32]. We have determined, according to Voxeur et al. 2019 [19], the relative amount of each oligogalacturonide (OG) comparing its peak area to the peak area of total OGs (sum of all areas) detected for each sample. Only the most abundant OGs, present as more than 1% of the total OGs, were plotted. With this method we cannot compare OGs between them, but we can emphasize the comparison, for a given OG, between different conditions such as substrates, cultivars as well as enzymes used for digestions.

3. Result and discussion

3.1. Sequence analysis and phylogeny

V. dahliae encodes more than 40 putative pectinolytic enzymes. Among them, 30 PLs and PNLs (belonging to PL1, PL3 and PL9 families), 9 PGs (including putative endo and exo) and 4 PMEs. We first performed phylogenetic analysis and compared Verticillium PGs and PMEs protein sequences with selected bacterial, fungal, insect and plant enzymes. The 18 PMEs clustered into five clades with plant PMEs (carrot DcPME, orange CsPME3 and tomato SlPME) in a distinct clade, as well as insect rice weevil PME (SoPME) (**Fig. 1A**). VdPME1 appears to be closely related to the two other PMEs from Aspergillus species, which are recognized as non-processive PMEs in their mode of action. VdPME1 showed 51.23 % and 51.08 % sequence identity with AaPMEI [33] and AnPMEI [34], respectively. As shown on **Fig. 1B** PGs, comprising 28 sequences, which clustered in seven clades allowing clear separation between putative endo and exo PGs from *V.dahliae* (VdPG 02879, VdPG 03463, VdPG 05992, VdPG 07608 VdPG 00768, VdPG 01781, VdPG G08089) with endo VdPG2 (04977). The plant PGs from *D. carota* (DcPG) and *A. thaliana* PGs (AtPGLR) clustered in a separated clade as well as PGs from yeast *S. cerevisiae* (ScPGUI) and fungal *C. purpureum* PG1 (CpPG1). VdPG2 forms an independent clade with fungal PGs from *C. lupini var. setosum* (ClPG1. 68.14 % sequence identity) which was shown to be endo-PGs [35].

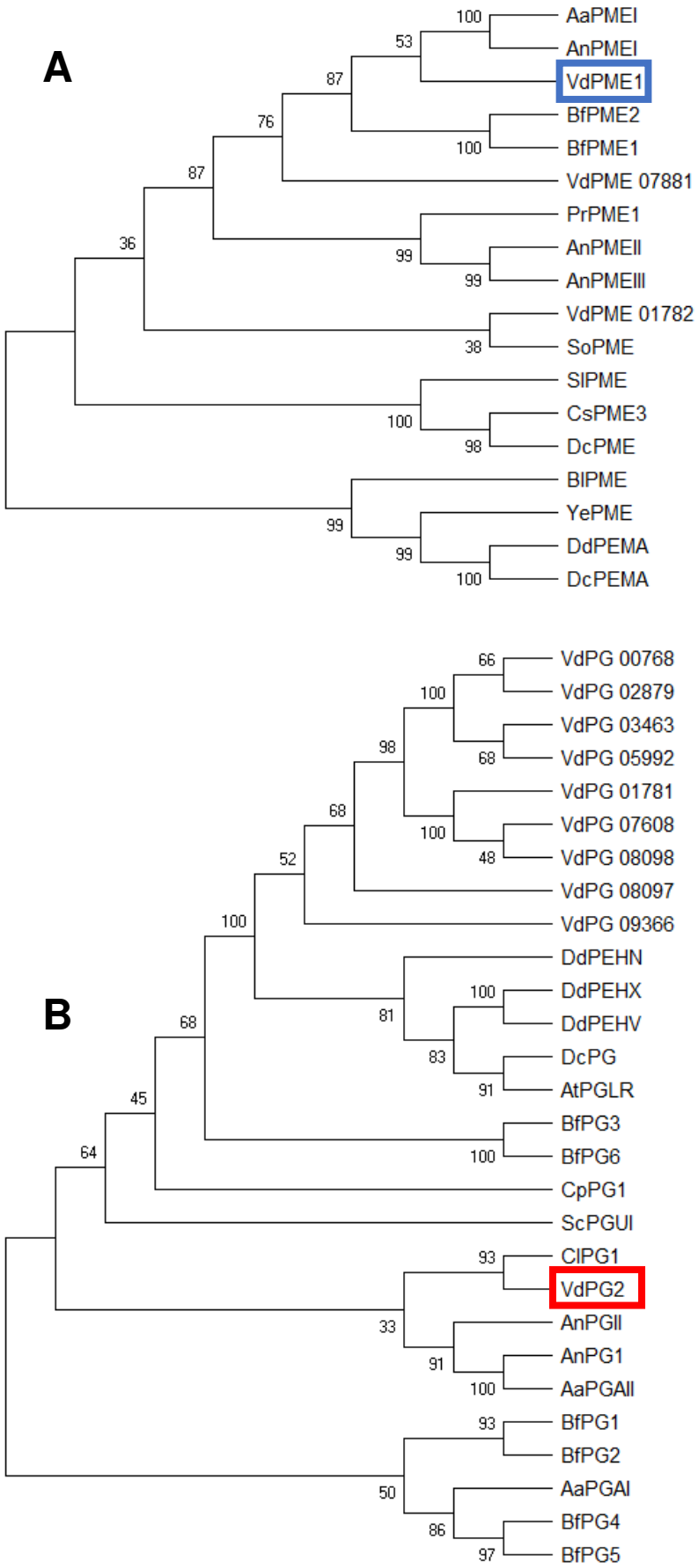

270

271 **Fig. 1. Phylogenetic relationships of VdPME1 and VdPG2 with selected fungal and bacterial**
272 **enzymes.**

Phylogenetic tree for PMEs (A) and PGs (B) *V. dahliae* PG2 (VdPG2, **VDAG_04977**) and PME1 (VdPME1, **VDAG_05799**) are red and blue-boxed, respectively. Amino acids sequences used are the following: *V. dahliae* PMEs (VDAG_07881, VDAG_1782) and *V. dahliae* PGs (VDAG_00768, VDAG_01781, VDAG_02879, VDAG_03463, VDAG_05992, VDAG_07608, VDAG_08097, VDAG_08098, VDAG_09366). *B. licheniformis* PME (Q65F39). *D. dadantii* PEHN (E0SDX9), PEHX (E0SKR4), PEHV (E0SKR2), PEMA (P0C1A9). *D. chrysanthemi* PEMA (P0C1A8). *Y. enterocolitica* PME (A1JJ76). *C. purpureum* PG1 (P79074) *B. fuckeliana* PGI (Q4G496), PG2 (Q4G495), PG3 (Q9Y7V9), PG4 (Q9Y7W0), PG5 (Q9Y7W1), PG6 (Q9Y7W2), PME1 (A0A384JQ57), PME2 (A0A384JCI5). *A. aculeatus* PGAI (O74213), PGAII (Q70HJ4), PMEI (Q12535). *A. niger* PGI (P26213), PGAII (P26214), PMEI (P17872), PMEII (G3YAL0), PMEIII (A0A345K402). *P. rubens* PME1 (B6HGX6). *C. lupini var. setosum* PG1 (A1E266). *S. cerevisiae* PGUI (P47180). *S. oryzae* PME (E7CIP7). *D. carota* PME (P83218), PG (Q75XT0). *S. lycopersicum* PME (P14280). *C. sinensis* PME3 (P83948). *A. thaliana* PGLR (Q9LYJ5). The maximum-likelihood tree was deduced from the genetic distances between aligned amino-acid sequences using MEGA. UniProt accession numbers were used.

3.2. Homology modelling and structure analysis

To fully understand the structural features of VdPG2 and VdPME1, their structures were modelled using the I-TASSER server for protein structure prediction. VdPME1 model was created using *D. carota PME* (P83218, PDB:1GQ8, [36]) as the template, with 31.42 % amino acid (AA) identity and 46.6 % similarity. Although VdPME1 doesn't share a high degree of identity with its template, the modelling remarkably provided a structure with a root mean square deviation (RMSD) of only 4.1±2.8Å. The model consisted of 314 AA, without the 16 AA of the signal peptide. Modelling shows that the enzyme is a right handed β-helix (**Fig. 2A**) structure that shares four highly conserved regions, as well as key active site residues characterized in other PMEs. These four regions comprise one N terminal region (Gly47, Ser48, Tyr49, Ala50 and Glu51), two internal regions (Tyr166-Phe166 (mutation in VdPME1) Gly167, Asp168, Thr169 and Asp165, Phe166, Ile167, Phe168 and Gly169) and one C-terminal region (Leu227, Gly228, Arg229, Pro300 and Trp301) [37]. The AA of the active site are Gln143, Asp144, Asp165 and Arg229 (**Fig. 2B, Fig. S1**) where the two Asp act as a general acid/base in the catalytic mechanism [18,38]. The VdPME1 showed high structural superposition with *D. dadantii, A. niger* and *D. carota* PMEs (PDB code 2NT6, 5C1C, 1GQ8, **Fig. 2C**).

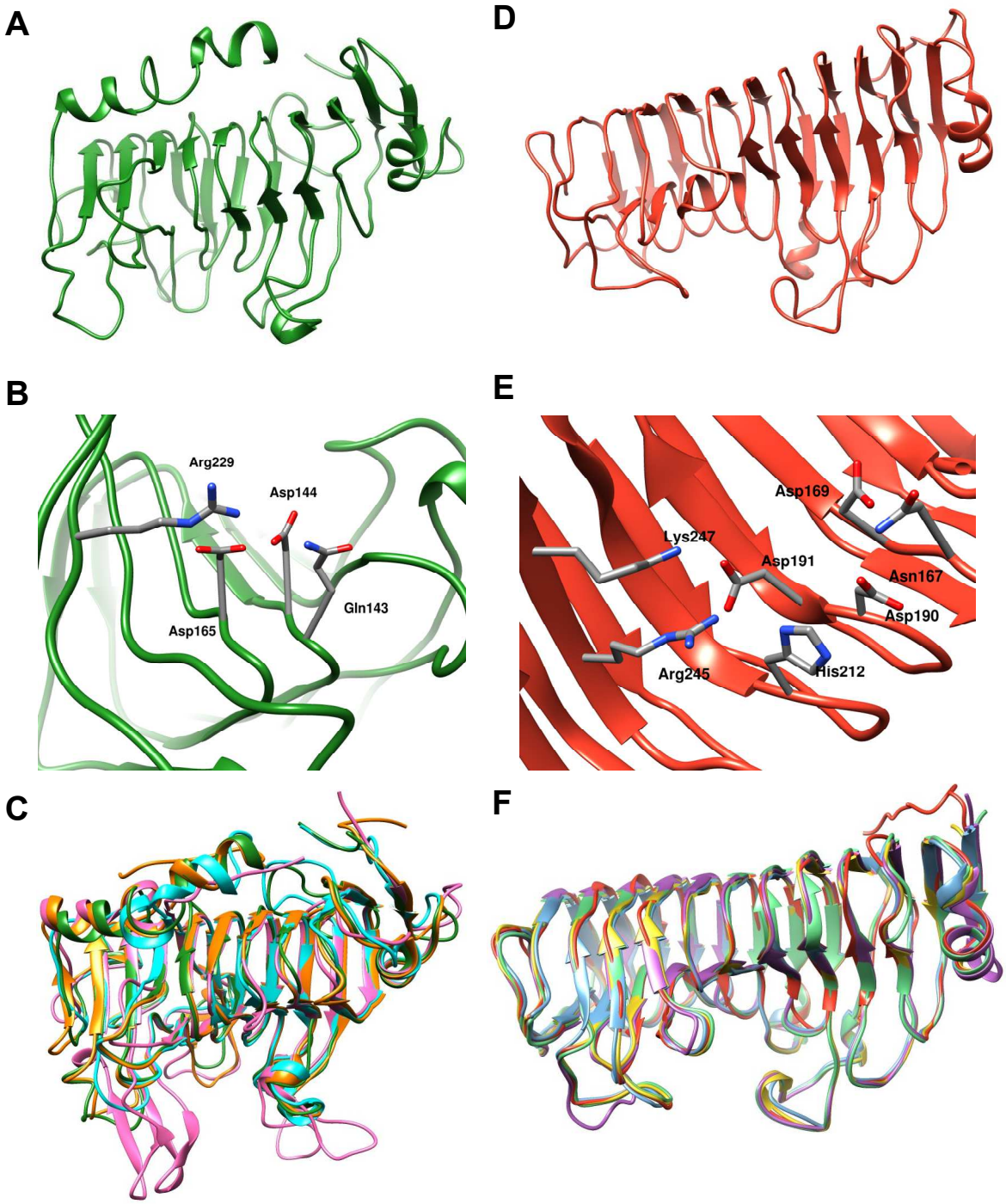

306

307 **Fig. 2. Homology modelling and structural comparison of VdPME1 and VdPG2**.

308 (A) VdPME1 homology model created using I-TASSER. (B) Structure of the active site of VdPME1.
309 Gln-143, Asp-144, Aps-165 and Arg-229 (VdPME1 numbering) are coloured in grey. (C) Structural
310 alignment of VdPME1 with crystalized enzymes from *D. carota* (DcPME, orange, PDB code 1gq8), *D.*
311 *dadantii* (DdPME, pink, PDB code 2nt6) and *A. niger* (AnPME, cyan, PDB code 5c1c). (D) VdPG2
312 homology model created using I-TASSER. (E) Structure of the active site of VdPG2. Asn-167, Asp-
313 169, Aps-190 and Aps-191, His-212, Arg-245, Lys-247 (VdPG2 numbering) are colored in grey. (F)
314 Structural alignment of VdPG2 PGs with crystalized enzymes from *A. niger* (AnPGII, bleu, PDB code

1czf), *A. niger* (AnPGI, green, PDB code 1nhc), *A. acuelatus* (AaPG, purple, PDB code 1ia5) and *C. lupini* (ClPG1, yellow, PDB code 2iq7, A1E266).

The VdPG2 model was created using *A. acuelatus* PGAI (O74213, PDB:1IA5, [39] as a best template with an estimated RMSD of 5.6±3.5Å. VdPG2 exhibits lower sequence identity with AaPGAI (55.74 %) compared to ClPG1 (68.14 %) but higher structural homology. The final model consists of 352 AA without the 18 AA of the signal peptide. The structure is a right handed β-helix with 10 complete turns (**Fig. 2D**). Members of GH28 family, including endo and exo PGs have conserved AA motifs, including Asn167, Thr168, Asp169 (NTD) Asp189, Asp190 (DD), Gly211, His212, Gly213 (GHG), Arg244, Ile245, Lys246 (RIK, **Fig. 2E**, **Fig. S2**, [40,41]) in VdPG2. Structural alignment with published PGs structures [35,39,42]confirmed that VdPG2 is likely to be an endo-PG with a tunnel like active cleft (**Fig. 2F**). Furthermore, while the catalytic amino acids are strongly conserved, tunnel like active cleft having the same shape differ in size, specifically regarding the size of the substrate which could be accepted [42].

3.3. Cloning, expression and purification of VdPG2 and VdPME1

The *VdPG2* (VDAG_04977) and *VdPME1* (VDAG_05799) genes consisting of 1113 and 993 bp, respectively; were amplified using gene specific primers without the signal peptide (**Table 1**), ligated in pPICZαB vector, expressed in *P. pastoris* and secreted in the culture media. The open reading frame consisted of 384 and 343 AA for VdPG2 and VdPME1, respectively, containing the poly-histidine tag for affinity chromatography purification. Following purification, VdPME1 and VdPG2 were resolved on SDS-PAGE, having an apparent molecular mass of ~ 39 and 50 kDa, respectively (**Fig. 3A, 4A**). The observed molecular mass is slightly higher compared to the predicted mass of 36.5 and 39.7 kDa, which could be related to the presence of two (Asn84, Asn201) and five (Asn122, Asn199, Asn220, Asn232, Asn331) potential N-glycosylation sites in VdPME1 and VdPG2, respectively. Additional O-glycosylation sites were predicted in VdPME1. The occurrence of glycosylation was confirmed through digestion with PNGase, leading to the expected shift in molecular mass for both enzymes (**Fig. S3**).

3.4. Biochemical characterization of VdPME1

Although PMEs from different species catalyse the same reaction, they can differ in their pH and temperature optima, substrate specificities and processivity [43]. VdPME1 exhibited the highest activity on moderately methylesterified citrus pectin (DM 55-70 %, **Fig. 3B**), albeit an activity was also detected on a wide range of pectic substrates that varied in their DM. VdPME1 activity was 68 % of the maximum on sugar beet pectin of DM 42 %, 53 % on citrus pectin of DM >85 % and 29 % on citrus pectin of DM 30 %; suggesting that VdPME1 acts preferably on moderate DM. This is in accordance with the results described for PME from *A. niger* [44] and *B. licheniformis* PME [45]. Furthermore, while citrus (DM 55-70 %) and apple (DM 70-75 %) pectins have slightly different DM, the differences in activity could result from distinct patterns of methylesterification or xylose linkages (higher amount in apple pectin,[46]) which could reduce the accessibility to the substrate [47]. When using citrus pectin DM 55-70 % as substrate, VdPME1 was active over a broad range of pH (**Fig. 3C**). While the maximum relative activity is at pH 6, residual activities were 95 % and 72 % at pH 5 and 7, respectively. pH optimum contrasted with that of fungal PMEs, AaPMEI (pH 4.5) [33], AnPMEII (pH 4.5) [38], plant DcPME (pH 7.5) [48], and orange CsPME3 (pH 7) [49].Temperature optimum, assessed using citrus DM 55-70 %, was 40 ˚C (**Fig. 3D**). The activity of VdPME1 drastically declined when not at optimal temperature with 40 % and 30 % of maximum activity at 50 ˚C and 30 ˚C, respectively. Similar values were reported for *P. chrysogenum* F46 PME (40 ˚C) [50], *A. niger* ZJ5 PME (45 ˚C) [44] and CsPME3 at (50 °C) [49]. Salt dependency of VdPME1 activity was determined using 0 to 300 mM NaCl (**Fig. S4**). Non-substantial effect was observed when using 0 to 50 mM concentration, while the residual activity was 50 % and 24 % at 100 mM and 300 mM NaCl, respectively. In that respect, as NaCl had no positive effect on activity, VdPME1 appears to be a salt-independent PME [43], as opposed to previously reported fungal AaPMEI [33] where salt increased the activity. Therefore, although of fungal origin, VdPME1 is more similar to Valencia orange peel PME where no salt is needed for the activity [51].The enzymatic parameters were determined using citrus pectin DM 55-70 % as a substrate. K_m and V_{max} were 3.27 ± 0.16 mg. mL^{-1} and 89.91 ± 1.39 nmol of MeOH.min^{-1}. μg^{-1} of proteins respectively (**Table S1**). These K_m values show a high affinity for the substrate, and are comparable to that of *A.niger* ZJ5 (AnPMEIII, 3.27 mg.mL^{-1}) [44] with higher V_{max} values (5.63 nmol of MeOH.min^{-1}.μg^{-1}). In contrast, the V_{max} are much lower than AaPMEI (5500 nmol of MeOH.min^{-1}.μg^{-1}) [33].

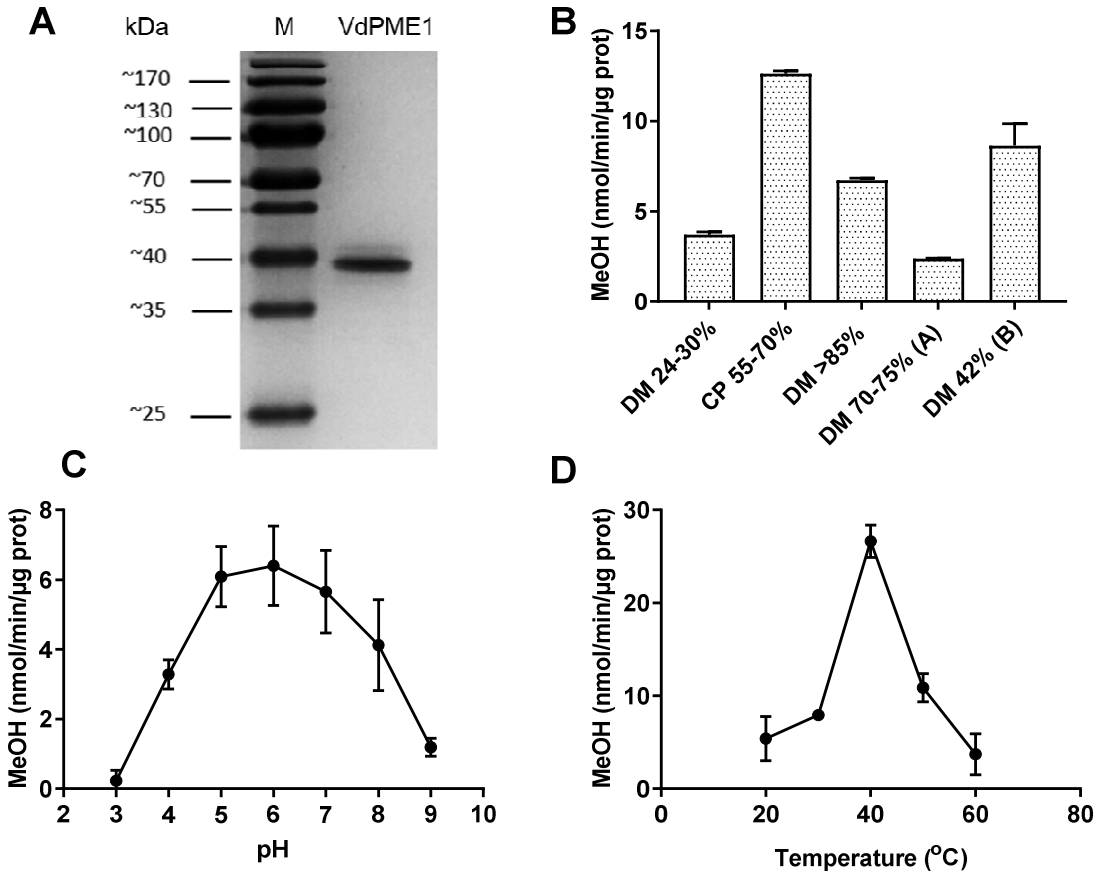

Fig. 3. Biochemical characterization of *Vd*PME1.

(A) SDS-PAGE analysis of VdPME1 following His-tag affinity purification. The gel was stained with Coomassie blue. The band at ± 34 kDa, corresponds to His-tagged and multiple bands corresponds to differently N-glycosylated forms of the purified enzyme. (B) Substrate specificity of VdPME1: Activity of VdPME1 was measured on pectic substrates of distinct DM and DA. Activity was measured at pH 7.5 using the alcohol oxidase coupled assay (C) Influence of the pH on VdPME1 activity. Activity was measured using sodium acetate (pH 3-5) and Tris-HCl (pH 6-9) buffer. (D) Influence of the temperature on VdPME1 activity. Activity was measured on pectins 55 %-70 % DM, pH 7.5 using the alcohol oxidase assay. The values are calculated as a MeOH released in as nmol of MeOH.min^{-1}.μg^{-1} of proteins. Data represent mean ± SD of three replicates.

3.5. Biochemical characterization of VdPG2

VdPG2 was most active on PGA (**Fig. 4B**) and its activity was negatively correlated with increasing the DM of pectins. A number of fungal, bacterial and plant PG show similar trend [52–54]. VdPG2 residual activity was 57 % on citrus pectin DM 30 %, and 34 % on citrus pectin DM 55-70 %. Similar biochemical characteristics were

described for *A. luchuensis* PGA B [55] and *P. occitanis* PG2 [56]. The activity of VdPG2 was close to null on sugar beet pectin which could be explained by the overall structure and acetylation patterns of the substrate, which could impair PG activity [4]. Using PGA as a substrate we showed that the optimal VdPG2 activity was at pH 5 (**Fig. 4C**), while at pH 6 and pH 7 only 14 % and 49 % of the activity measured at pH 5 were detected, respectively. This is similar with the previously reported fungal acidic pectinase BfPG1 and BfPG2 (pH 4.2 and 4.5) that also showed high sequence similarity to VdPG2 [54]. In contrast, the optimal pH for VdPG2 was slightly higher to that of *C. pteridis* PG activity on (pH 4) [57], *A. acuelatus* PG (pH 4.5) [58] and *S. purpureum* PG (pH 4.5) [59]. Temperature optimum was at 50°C (**Fig. 4D**), with 90 % and 78 % residual activities at 40 °C and 30 °C, respectively. Above 50 °C there was a sharp decline in activity. These temperatures optimums (40-50 ˚C) were previously reported for a number of fungal, insect and plant PGs [4,32,55]. In contrast *F. palustris* and *S. purpureum* PGs were most active at 60 ˚C [59,60]. The enzymatic parameters were calculated using PGA as a substrate (**Table S1**). K_m and V_{max} were 8.34 ± 0.74 mg. mL^{-1} and 40.28 ± 1.2 µmol of GalA min^{-1}. $µg^{-1}$ of proteins respectively. This is in the range of previously reported values for fungal PGs [12].

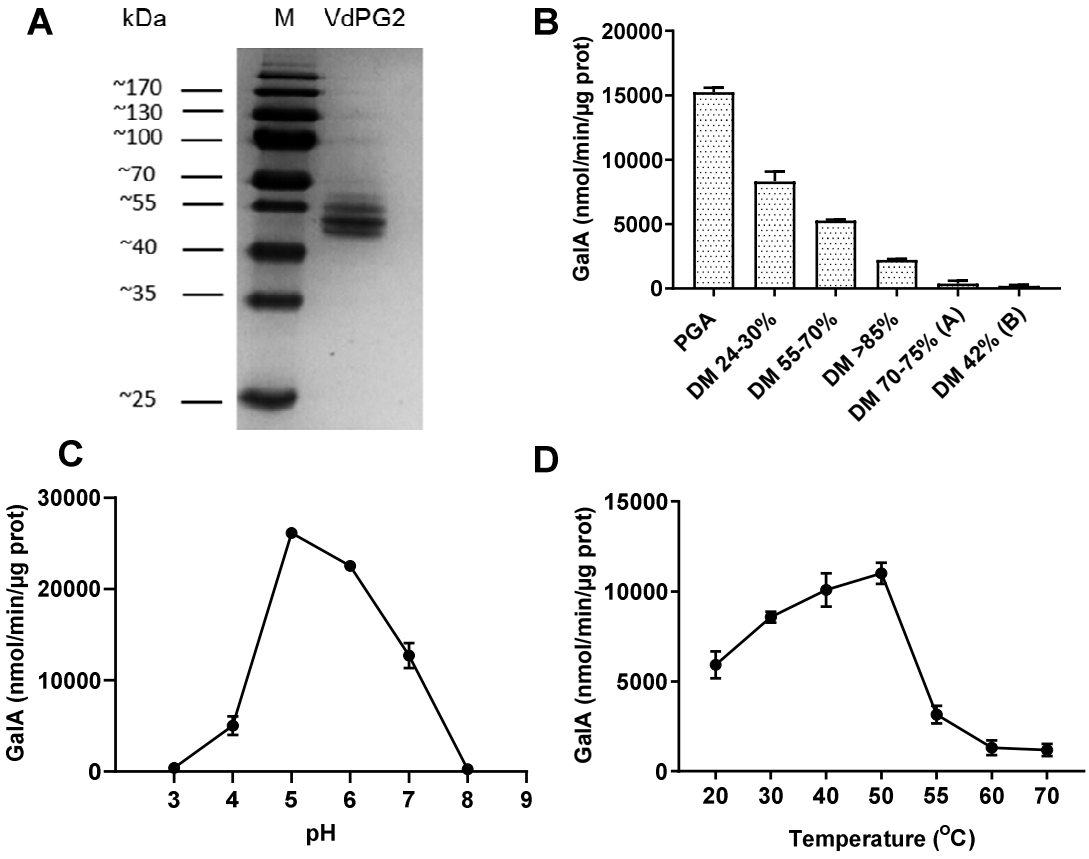

416

417 **Fig. 4. Biochemical characterization *of* PG2.**

418 (A) SDS-PAGE analysis of VdPG2 following His-tag affinity purification. The gel was stained with
419 Coomassie blue and the bands at 38 kDa corresponds to His-tagged and multiple bands correspond
420 to differently N-glycosylated forms of the purified enzyme. (B) Substrate specificity of VdPG2. Activity
421 of VdPG2 was measured on PGA and pectic substrates of distinct DM and DA. Activity was measured
422 at pH 5 using the DNS method. (C) Influence of the pH on VdPG2 activity. Activity was measured on
423 PGA at 50 °C using the DNS method (D) Influence of the temperature on VdPG2 activity. Activity was
424 measured on PGA, pH 5 using the DNS method. The values are calculated as a nmol of GalA min^{-1}.μg^{-1} of proteins. Data represent mean ± SD for three replicates.

426 ### 3.6. Identification of the OGs released VdPG2

427 The analysis of the digestion products of PG is a key to understand the diversity of
428 this family of enzymes and assess the potential role of the various isoforms. Using a
429 recently developed LC-MS approach [19], OGs released by VdPG2 were identified
430 after digestion of citrus pectin of various DM. When digesting citrus pectin of DM 20-
431 34 % (**Fig. 5A, DM 20-34 %, Fig. S6A**) the majority of released OGs were non-
432 methylesterified OGs, of DP 3 and 2 ($GalA_3$ 47.67 % and $GalA_2$ 16.63 % of total OGs

433 detected). Moreover, $GalA_3$ and $GalA_2$ were not cleaved and accumulated during the
434 reaction, as in order to hydrolyse them, the enzyme would have to fold into
435 unfavourable conformation [61]. Other OGs were methylesterified GalA of DP 3 and 4
436 ($GalA_4Me$ 12.88 % and $GalA_3Me$ 8.70 %). Altogether, these four OGs represented
437 85.89 % of all detected OGs. $GalA_6Me_2$, was the OG with the highest DP detected.
438 This shows that VdPG2 act as an endo enzyme, in contrast to exo-PGs which
439 release mostly GalA products [40]. When using a more methylesterified substrate
440 (DM 55-70 %), the $GalA_3$ was still the most abundant OG (20.49 %) with a relative
441 abundance of $GalA_4Me$ and $GalA_3Me$ of 12.82 % and 11.82 % (**Fig. 5A, DM 55-70**
442 **%, Fig. S6B**), respectively. Furthermore, additional methylesterified OGs of DP7 and
443 DP8 were detected ($GalA7Me_2$, $GalA7Me_3$, $GalA8Me_4$). Interestingly, when digesting
444 the citrus pectin DM 55-70 % increase of non-methylesterified OGs is observed,
445 notably $GalA_4$ (8.88 %) and $GalA_6$ (3.78 %). This could be due to the random
446 distribution of methyls in HG chain coupled with single-attack (non-processive) nature
447 of VdPG2 which cloud lead to increased release of non-methylesterified OGs.
448 $GalA_3Me$, $GalA_4Me$ and $GalA_2$ were the most abundant OGs identified after digestion
449 of citrus pectins of DM >85 %, with 19.66 %, 16.07 % and 13 %, respectively (**Fig.**
450 **5A, DM >85 %**, **Fig. S6C**). In contrast the relative amount of $GalA_3$ was drastically
451 reduced to 10.37 % (of total OGs detected), and 74.14 % of all OGs were
452 methylesterified. Overall VdPG2 released 66.56 % of non-methylesterified OGs from
453 citrus pectin DM 20-34 % and 25.86 % from pectins of DM >85 % (**Fig. 5B**). These
454 OGs represent the final products after 24 h digestion and it can be assumed that they
455 cannot be further hydrolysed due to unfavourable methyl substitutions. This was
456 tested by analysing the OGs released following 15, 45, 90 and 180 min incubation,
457 with DM 24-30 %, where no differences between various incubation times were
458 observed (**Fig. S5**).

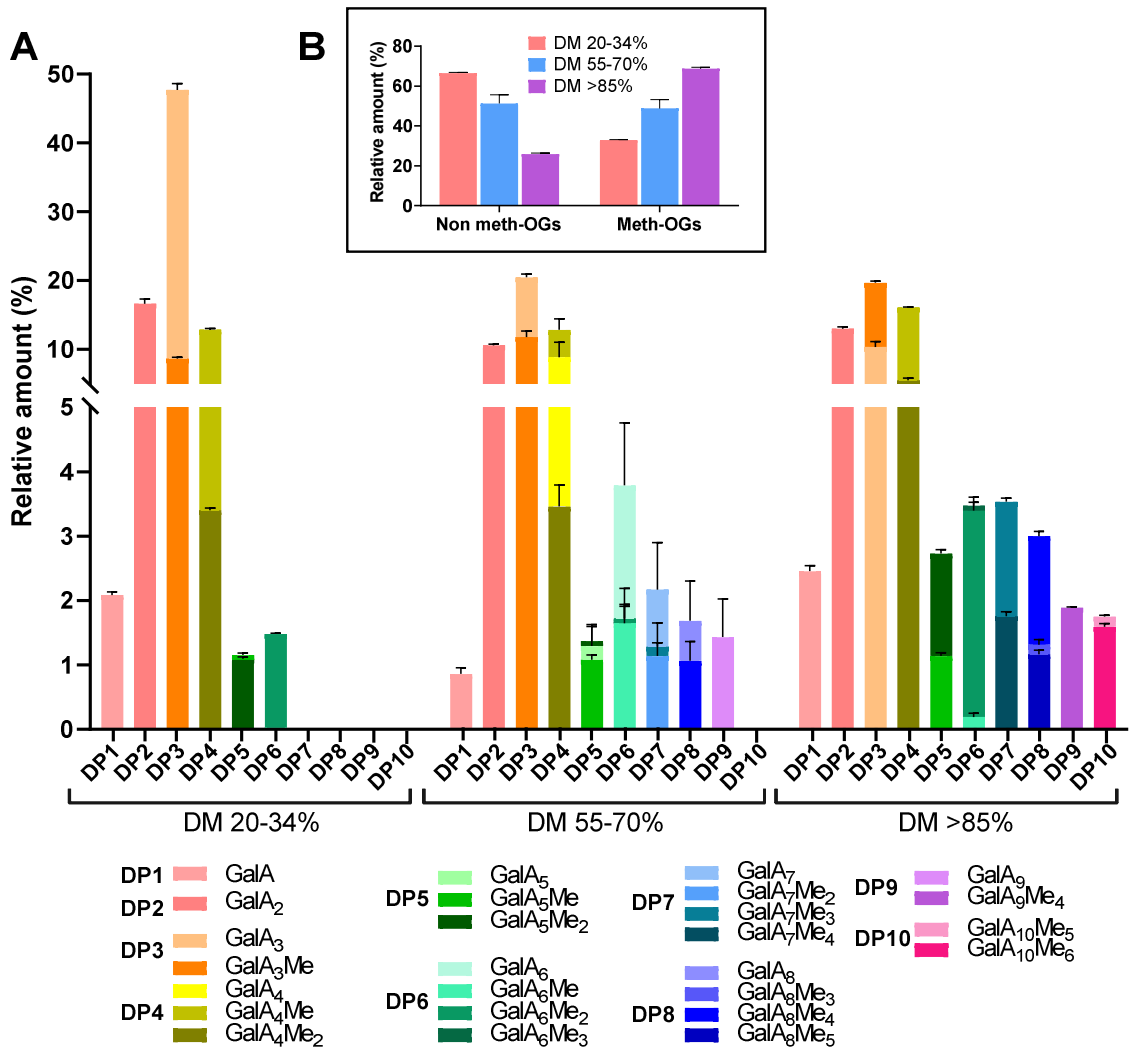

Fig. 5. HP-SEC-MS analysis of OGs released by VdPG2 after over-night incubation with citrus pectins.

(A) OGs released by activity of VdPG2 on pectins of distinct DM (20-34 %, 55-70 % and >85 %) were separated using SEC and analysed using MS/MS. OGs are represented according to their DP and DM. Figure shows 88.5 % (DM 20-34 %), 80 % (DM 55-70 %) and 82.6 % (DM >85 %) of total OGs detected. (B) Total of the non-methylesterified and methylesterified OGs. Data are means ± SD; n = 3. Subscript numbers indicate the DP and DM.

As a means of comparing the mode of action of VdPG2 with previously characterized PG, the digestion profile of AaPGM2, a commercial endo-PG M2 from *Aspergillus aculeatus*, was compared with that of VdPG2. Citrus pectin with DM 20-34 % and DM 55-70 % were digested during 2 hours with each of the enzymes and the released OGs were compared (**Fig. S7**). Overall, both enzymes released the same OGs in different relative quantities. Differences came from the abundance of non-

473 methylesterified $GalA_3$ (17 % for AaPGM2 vs 47 % VdPG2) and the absence of
474 $GalA_4Me_2$ detected following AaPGM2 digestion of pectin DM 20-34 % (**Fig. S7A)**.
475 Higher differences were detected with pectin DM 55-70 % (**Fig. S7B**), where
476 AaPGM2 releases OGs of higher DP with complex methyl substitutions. This further
477 reinforce the previous statement that VdPG2 has less affinity for pectins with complex
478 methylesterification patterns compared to AaPGM2. The mode of action of these two
479 enzymes differ and probably these differences are likely to be dependent on the
480 active site subsites, as reported for AnPGII, where the Glu252Ala mutation increased
481 the activity of the enzyme on partially methylesterified substrate [62]. That specific AA
482 is different for two enzymes (Asp259, VdPG2 numbering) which could explain this
483 distinct behaviour, but AA at other subsites should be also considered when
484 determining enzyme specificity.

485 **3.7. VdPME1 has a processive mode of action**

486 As a way to determine the mode of action of VdPME1, we first digested moderately
487 methylesterified substrate citrus pectin DM 55-70 % for 2 hours using VdPG2 (**Fig.**
488 **6A**). This led to the release of methylesterified and non-methylesterified OGs. This
489 pool of OGs was subsequently used as substrate for determining the mode of action
490 of VdPME1 at pH 7 after 15 min and overnight digestion. LC-MS/MS oligoprofiling
491 showed that for the two incubation times, only non-methylesterified GalA, $GalA_2$ and
492 $GalA_3$ were detected (**Fig. 6B**).

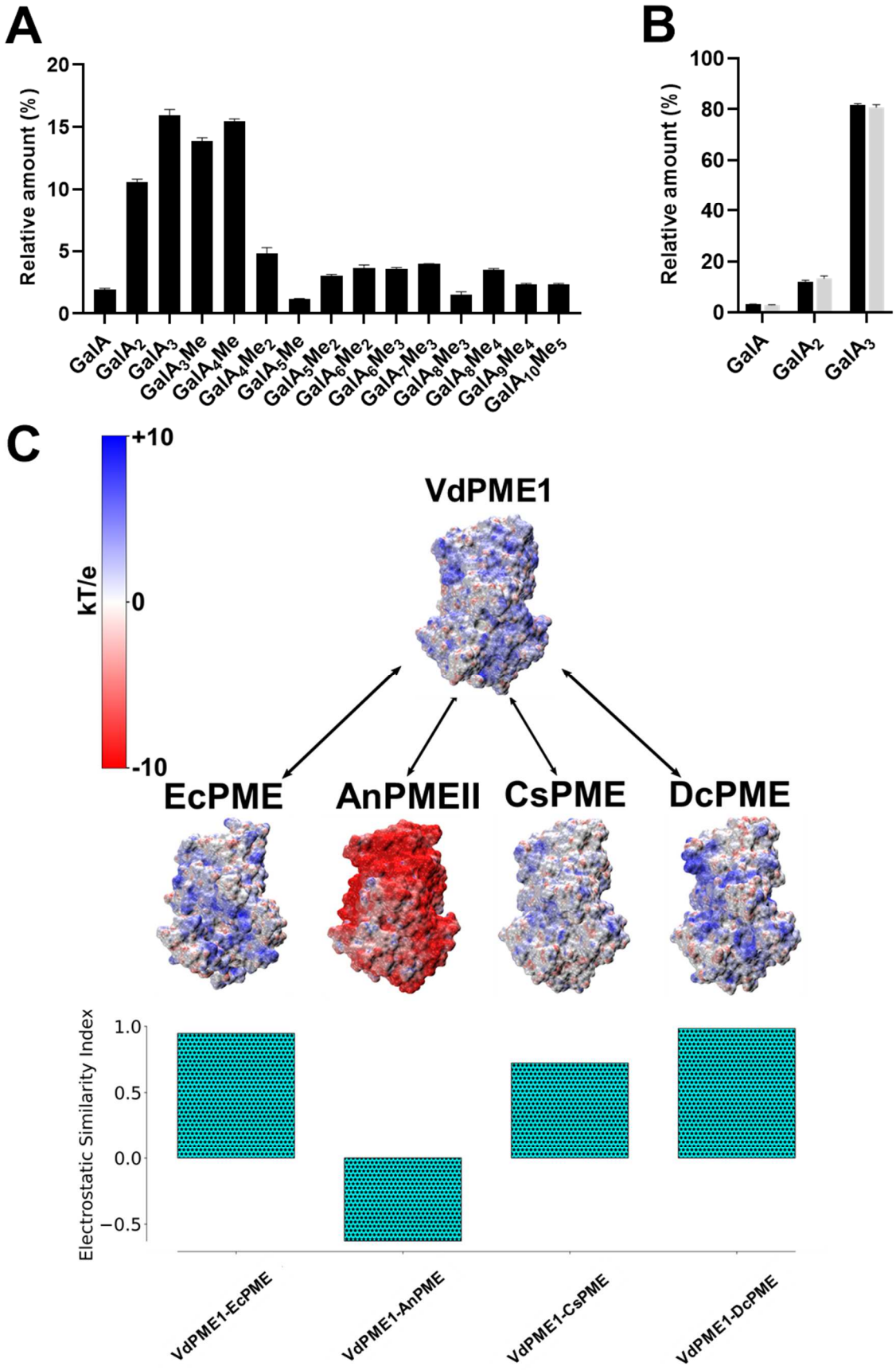

493

494 **Fig. 6. Mode of action and electrostatic potential of VdPME1**

(A) Population of OGs of various DP and DM generated by action of VdPG2 during 2 h at 37 °C on pectin DM 55-70 % (B) OG produced from the "VdPG2-population" after 15 min (black) and overnight incubation (grey) with VdPME1. Only mono-, di-, tri- galacturonic acids were identified. Data are means ± SD; n = 3. Subscript numbers indicate the DP and DM. (C) Electrostatic potentials, projected on the enzyme surface, calculated for *Verticillium dahliae* (VdPME1), *Dickeya dadantii* (DdPME), *Citrus sinensis* (CsPME) and *Daucus carota* (DcPME) PMEs at pH 7.0. Positive and negative regions of the potential are coloured from blue to red with a scale ranging between -10 and +10 kT/e. Pairwise similarity indices calculated to understand the resemblance of electrostatic potentials between the PME from *Verticillium dahliae* (VdPME1) and the other PMEs are shown as bars in the lower panel. A similarity index of +1.0 shows correlated electrostatic potentials (high similarity – see methods for more details), whereas a value of -1.0 shows anti-correlated potentials. Any value in between shows different to no correction (similarity index = 0).

Together, these data show that VdPME1 can produce long stretches of non-methylesterified GalA that have been, in the context of the experiment, further hydrolysed by the still-active VdPG2. Processive PMEs have been reported to have a neutral to alkaline optimal pH while non-processive PMEs are active at acidic pH [38]. It has been shown that *A. niger* PMEII, (AnPMEII) that has an optimal pH at 4.5 is a non-processive, while orange (CsPME), carrot (DcPME) and *D. dadantii* (DdPME) PMEs were shown to be processive at pH 7.5 [38,63]. Considering the importance of the electrostatic properties in defining substrate specificity and processivity [17], we have performed a quantitative analysis of the electrostatic properties of the modelled VdPME1 and compared those to what is known for other well-characterised PMEs. As shown on the **Fig. 6C** the comparison highlights a clear difference with the acidophile AnPMEII with electrostatics characterising the binding grooves being of opposite signs (a strong negative electrostatic potential for AnPMEII, and a strongly positively charged group for VdPME1 at pH 7.0). The electrostatic potential of VdPME1 is similar to that of the CsPME and DcPME, known to be processive at neutral pH, with an overall positive charge and a similarity index close to 1.0. This contrasted with the negative electrostatic potential of AnPMEII which can facilitate the dissociation of the enzyme-substrate complex for highly de-methylesterified substrates, which have a strong negative charge and anticorrelated similarity index. The relation between the electrostatic properties of the binding groove and processivity could be explained on the basis of simple electrostatics, with the repulsion between carboxylate groups of HGs and negatively charged residues in the binding groove being a determinant for low affinity. Nevertheless, residue-specific

preferences for different methylation or acetylation states for the substrate in specific subsites along the binding groove are most likely important to quantitatively tune processivity among PMEs showing processive behaviour.

3.8. Two Verticillium-sensitive and tolerant cultivars differ in their root pectin structure

Phytopathogenic fungi use pectinolytic enzymes, including PGs, PMEs, PLLs during infection to degrade pectins [64]. *V. dahliae* as a soilborne pathogen attacks flax root to infect the plants. In order to determine the contribution of VdPG2 in degrading flax cell wall we digested roots cell wall of two flax cultivars Évéa (*Verticillium*-partially resistant), and Violin (*Verticillium*-susceptible) with VdPG2. VdPG2 showed activity on flax roots and OGs up to DP6 were detected (**Fig. 7**). In particular, VdPG2 released non-methylesterified (GalA, $GalA_2$, $GalA_3$, $GalA_4$) and methylesterified ($GalA_3Me$ and $GalA_4Me$, in both cultivars, approx. 1.5 %) OGs which have been previously identified from commercial pectic substrates. In addition, VdPG2 released acetylated substrates, $GalA_3Ac$, $GalA_4Ac$, $GalA_4Ac_2$, showing that the enzyme is able to hydrolyse acetylated pectins. $GalA_4MeAc$ was the only methylesterified and acetylated OG detected. It appears that VdPG2 has lower affinity for pectic population having acetyl and methyl groups. In particular, the distribution of methyl and acetyl groups on HGs was shown to have an impact on enzyme substrate interaction, as acetylation of HGs strongly change the association of enzyme on substrate [65]. Overall, following digestion by VdPG2, both genotypes, Évéa and Violin, produced similar diversity and relative abundance of OGs (**Fig. 7**) except for $GalA_3Me$, which was specifically detected in Évéa, the *Verticillium*-partially resistant cultivar. This specific OG only produced from the roots of the resistant cultivar suggests that its cell wall structure differed to that of the susceptible cultivar. When *V. dahliae* infests flax roots, pectins digestion by PGs such as VdPG2 can lead to releasing OGs similar to the above-mentioned one. This could play a role in triggering distinct signalling events between resistant and susceptible cultivars. Indeed, previous reports show that small OGs, especially trimers could be involved in activation of genes involved in defence and phytohormone signalling, as well in the down-regulation of genes involved in growth regulation and development [66]. In addition, this OG could act as danger-associated molecular patterns (DAMPs) in flax

562 which would lead to activation of defence-related pathways, thus reducing the
563 susceptibility to pathogen infection [67].

564

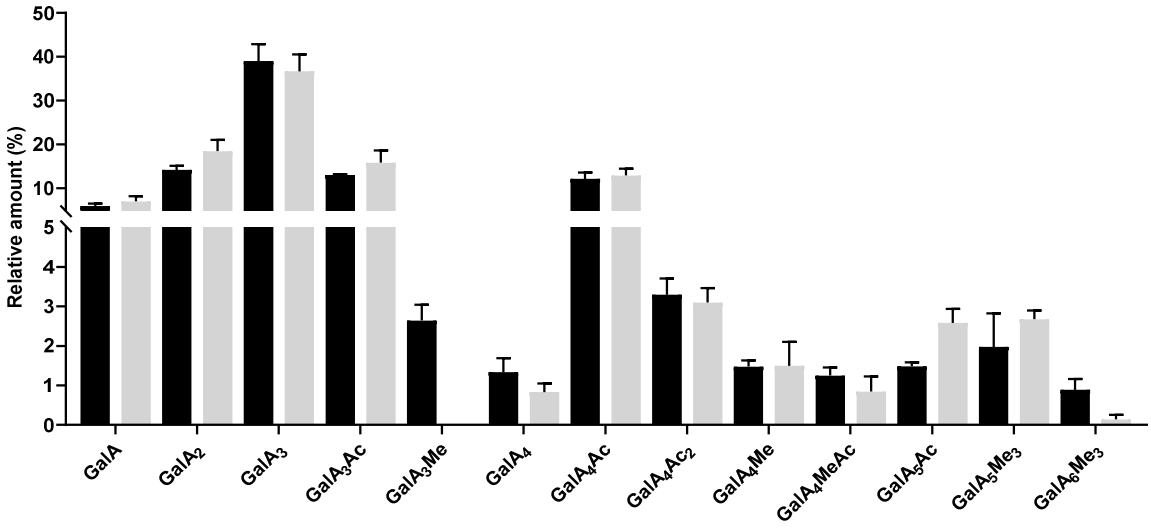

565

566 **Fig. 7. Analysis of OGs released by VdPG2 from flax roots.**

567 VdPG2 was incubated overnight with roots from Évéa (spring flax, partially resistant to Verticillium wilt,
568 black) and Violin (winter flax, more susceptible to Verticillium wilt, grey). Data are means ± SD; n = 3.
569 Subscript numbers indicate the DP and DM.

570

571 ## 4. Conclusion

572 We characterized two novel enzymes from *V.dahliae:* VdPME1 and VdPG2. They
573 show high activity on pectic substrates but also, for VdPG2, on cell wall pectins from
574 flax roots. Biochemical characteristics were determined for both enzymes which
575 showed, VdPG2 is an endo PG that can release methylesterified, non-
576 methylesterified and acetylated OGs, with preference for unsubstituted and slightly
577 substituted pectic populations. This, together with homology modelling suggests that
578 small differences in the enzyme structure could be of importance to determine the
579 substrate specificities. Model for VdPME1 shows similar structural features to that
580 reported for fungal and plant PMEs, but a surprising processive behaviour commonly
581 observed for plants PMEs. This processive behaviour could relate to the electrostatic
582 potential of the protein. The processive mode of action of VdPME1 could enable

583 release of pectins for which VdPG2 has a high affinity. This study shows that HP-
584 SEC-MS can be used as a method of choice for the detection and quantification of
585 OGs released by the action of VdPG2 and VdPME1 from commercial pectin and flax
586 root cell wall pectins. Moreover, synergistic properties of these two enzymes suggest
587 that VdPG2 and VdPME1 are important pectinolytic enzymes in *V.dahliae* arsenal.
588 This study may lead to new approach for the protection of crops against pathogens.

589

590 **Funding sources**

591 This work was funded by the Conseil Regional Hauts-de-France and the FEDER
592 (Fonds Européen de Développement Régional) through a PhD studentship awarded
593 for to J.S.

594

595 **CRediT authorship contribution statement**

596 **Josip Safran:** Conceptualization, Data curation, Formal analysis, Investigation,
597 Methodology, Writing - original draft**. Olivier Habrylo**: Formal analysis, Investigation,
598 Methodology. **Mehdi Cherkaoui**: Methodology. **Sylvain Lecomte**: Methodology.
599 **Aline Voxeur**: Methodology. **Serge Pilard**: Investigation, Methodology **Solène**
600 **Bassard**: Methodology **Corrine Pau-Roblot** Conceptualization, Investigation,
601 Methodology. **Davide Mercadante**: Conceptualization, Writing - review & editing
602 **Jérôme Pelloux**: Funding acquisition, Conceptualization, Writing - review & editing.
603 **Fabien Sénéchal**: Conceptualization, Writing - review & editing.

604

Reference

[1] N.C. Carpita, D.M. Gibeaut, Structural models of primary cell walls in flowering plants: consistency of molecular structure with the physical properties of the walls during growth, Plant J. 3 (1993) 1–30. https://doi.org/10.1111/j.1365-313X.1993.tb00007.x.

[2] B.L. Ridley, M.A. O'Neill, D. Mohnen, Pectins: Structure, biosynthesis, and oligogalacturonide-related signaling, 2001. https://doi.org/10.1016/S0031-9422(01)00113-3.

[3] D. Mohnen, Pectin structure and biosynthesis, Curr. Opin. Plant Biol. 11 (2008) 266–277. https://doi.org/10.1016/j.pbi.2008.03.006.

[4] O. Habrylo, D.E. Evangelista, P.V. Castilho, J. Pelloux, F. Henrique-Silva, The pectinases from Sphenophorus levis: Potential for biotechnological applications, Int. J. Biol. Macromol. 112 (2018) 499–508. https://doi.org/10.1016/j.ijbiomac.2018.01.172.

[5] V. Lionetti, E. Fabri, M. De Caroli, A.R. Hansen, W.G.T. Willats, G. Piro, D. Bellincampi, Three pectin methylesterase inhibitors protect cell wall integrity for arabidopsis immunity to Botrytis, Plant Physiol. 173 (2017) 1844–1863. https://doi.org/10.1104/pp.16.01185.

[6] C.S.L. Vicente, L.G. Nemchinov, M. Mota, J.D. Eisenback, K. Kamo, P. Vieira, Identification and characterization of the first pectin methylesterase gene discovered in the root lesion nematode Pratylenchus penetrans, PLoS One. 14 (2019) 1–19. https://doi.org/10.1371/journal.pone.0212540.

[7] R.S. Jayani, S. Saxena, R. Gupta, Microbial pectinolytic enzymes: A review, Process Biochem. 40 (2005) 2931–2944. https://doi.org/10.1016/j.procbio.2005.03.026.

[8] Y. Yang, Y. Yu, Y. Liang, C.T. Anderson, J. Cao, A Profusion of Molecular Scissors for Pectins: Classification, Expression, and Functions of Plant Polygalacturonases, 9 (2018) 1–16. https://doi.org/10.3389/fpls.2018.01208.

[9] G. Limberg, R. Körner, H.C. Buchholt, T.M.I.E. Christensen, P. Roepstorff, J.D. Mikkelsen, Analysis of different de-esterification mechanisms for pectin by

enzymatic fingerprinting using endopectin lyase and endopolygalacturonase II from A. Niger, Carbohydr. Res. 327 (2000) 293–307. https://doi.org/10.1016/S0008-6215(00)00067-7.

[10] I. Kars, M. McCalman, L. Wagemakers, J.A.L. Van Kan, Functional analysis of Botrytis cinerea pectin methylesterase genes by PCR-based targeted mutagenesis: Bcpme1 and Bcpme2 are dispensable for virulence of strain B05.10, Mol. Plant Pathol. 6 (2005) 641–652. https://doi.org/10.1111/j.1364-3703.2005.00312.x.

[11] R.G. Cameron, B.J. Savary, A.T. Hotchkiss, L. Fishman, H.K. Chau, R.A. Baker, K. Grohmann, Separation and Characterization of a Salt-Dependent Pectin Methylesterase from Citrus sinensis Var. Valencia Fruit Tissue, J. Agric. Food Chem. 51 (2003) 2070–2075. https://doi.org/10.1021/jf020933.

[12] S.K. Niture, Comparative biochemical and structural characterizations of fungal polygalacturonases, Biologia (Bratisl). 63 (2008) 1–19. https://doi.org/10.2478/s11756-008-0018-y.

[13] N. Liu, X. Ma, Y. Sun, Y. Hou, X. Zhang, F. Li, Necrotizing activity of Verticillium dahliae and Fusarium oxysporum f. Sp. Vasinfectum endopolygalacturonases in cotton, Plant Dis. 101 (2017) 1128–1138. https://doi.org/10.1094/PDIS-05-16-0657-RE.

[14] A. Ten Have, W. Mulder, J. Visser, J.A.L. Van Kan, The endopolygalacturonase gene Bcpg1 is required to full virulence of Botrytis cinerea, Mol. Plant-Microbe Interact. 11 (1998) 1009–1016. https://doi.org/10.1094/MPMI.1998.11.10.1009.

[15] E.F. Fradin, B.P.H.J. Thomma, Physiology and molecular aspects of Verticillium wilt diseases caused by V. dahliae and V. albo-atrum, Mol. Plant Pathol. 7 (2006) 71–86. https://doi.org/10.1111/j.1364-3703.2006.00323.x.

[16] A. Blum, M. Bressan, A. Zahid, I. Trinsoutrot-Gattin, A. Driouich, K. Laval, Verticillium Wilt on Fiber Flax: Symptoms and Pathogen Development In Planta, Plant Dis. 102 (2018) 2421–2429. https://doi.org/10.1094/PDIS-01-18-0139-RE.

[17] D. Mercadante, L.D. Melton, G.B. Jameson, M.A.K. Williams, Processive pectin

methylesterases: The role of electrostatic potential, breathing motions and bond cleavage in the rectification of brownian motions, PLoS One. 9 (2014) 1–11. https://doi.org/10.1371/journal.pone.0087581.

[18] M. Fries, J. Ihrig, K. Brocklehurst, V.E. Shevchik, R.W. Pickersgill, Molecular basis of the activity of the phytopathogen pectin methylesterase, EMBO J. 26 (2007) 3879–3887. https://doi.org/10.1038/sj.emboj.7601816.

[19] A. Voxeur, O. Habrylo, S. Guénin, F. Miart, M.C. Soulié, C. Rihouey, C. Pau-Roblot, J.M. Domon, L. Gutierrez, J. Pelloux, G. Mouille, M. Fagard, H. Höfte, S. Vernhettes, Oligogalacturonide production upon Arabidopsis thaliana-Botrytis cinerea interaction, Proc. Natl. Acad. Sci. U. S. A. 116 (2019) 19743–19752. https://doi.org/10.1073/pnas.1900317116.

[20] J. Wang, P. Cieplak, P.A. Kollman, How Well Does a Restrained Electrostatic Potential (RESP) Model Perform in Calculating Conformational Energies of Organic and Biological Molecules?, J. Comput. Chem. 21 (2000) 1049–1074. https://doi.org/10.1002/1096-987X(200009)21:12<1049::AID-JCC3>3.0.CO;2-F.

[21] T.J. Dolinsky, J.E. Nielsen, J.A. McCammon, N.A. Baker, PDB2PQR: An automated pipeline for the setup of Poisson-Boltzmann electrostatics calculations, Nucleic Acids Res. 32 (2004) 665–667. https://doi.org/10.1093/nar/gkh381.

[22] N.A. Baker, D. Sept, S. Joseph, M.J. Holst, J.A. McCammon, Electrostatics of nanosystems: Application to microtubules and the ribosome, Proc. Natl. Acad. Sci. U. S. A. 98 (2001) 10037–10041. https://doi.org/10.1073/pnas.181342398.

[23] C.R. Søndergaard, M.H.M. Olsson, M. Rostkowski, J.H. Jensen, Improved treatment of ligands and coupling effects in empirical calculation and rationalization of p K a values, J. Chem. Theory Comput. 7 (2011) 2284–2295. https://doi.org/10.1021/ct200133y.

[24] N. Blomberg, R.R. Gabdoulline, M. Nilges, R.C. Wade, Classification of protein sequences by homology modeling and quantitative analysis of electrostatic similarity, Proteins Struct. Funct. Genet. 37 (1999) 379–387. https://doi.org/10.1002/(SICI)1097-0134(19991115)37:3<379::AID-

PROT6>3.0.CO;2-K.

[25] R.C. Wade, R.R. Gabdoulline, F. De Rienzo, Protein interaction property similarity analysis, Int. J. Quantum Chem. 83 (2001) 122–127. https://doi.org/10.1002/qua.1204.

[26] D.B. Mitchell, K. Vogel, B.J. Weimann, L. Pasamontes, A.P.G.M. Van Loon, The phytase subfamily of histidine acid phosphatases: Isolation of genes for two novel phytases from the fungi Aspergillus terreus and Myceliophthora thermophila, Microbiology. 143 (1997) 245–252. https://doi.org/10.1099/00221287-143-1-245.

[27] A. Lemaire, C. Duran Garzon, A. Perrin, O. Habrylo, P. Trezel, S. Bassard, V. Lefebvre, O. Van Wuytswinkel, A. Guillaume, C. Pau-Roblot, J. Pelloux, Three novel rhamnogalacturonan I- pectins degrading enzymes from Aspergillus aculeatinus: Biochemical characterization and application potential, Carbohydr. Polym. 248 (2020) 116752. https://doi.org/10.1016/j.carbpol.2020.116752.

[28] G.L. Miller, Use of Dinitrosalicylic Acid Reagent for Determination of Reducing Sugar, Anal. Chem. 31 (1959) 426–428. https://doi.org/10.1021/ac60147a030.

[29] D. Castaldo, E. Al., Isolation and Characterization of Pectin Methylesterase from Apple Fruit, Enzyme. 54 (1989) 653–656.

[30] J.A. Klavons, R.D. Bennett, Determination of Methanol Using Alcohol Oxidase and Its Application to Methyl Ester Content of Pectins, J. Agric. Food Chem. 34 (1986) 597–599. https://doi.org/10.1021/jf00070a004.

[31] M. L'Enfant, P. Kutudila, C. Rayon, J.M. Domon, W.H. Shin, D. Kihara, A. Wadouachi, J. Pelloux, G. Pourceau, C. Pau-Roblot, Lactose derivatives as potential inhibitors of pectin methylesterases, Int. J. Biol. Macromol. 132 (2019) 1140–1146. https://doi.org/10.1016/j.ijbiomac.2019.04.049.

[32] L. Hocq, S. Guinand, O. Habrylo, A. Voxeur, W. Tabi, J. Safran, F. Fournet, J.-M. Domon, J.-C. Mollet, S. Pilard, C. Pau-Roblot, A. Lehner, J. Pelloux, V. Lefebvre, The exogenous application of At PGLR, an endo -polygalacturonase, triggers pollen tube burst and repair, Plant J. (2020) 1–17. https://doi.org/10.1111/tpj.14753.

[33] S. Christgau, L. V Kofod, T. Halkier, L.N. Andersen, M. Hockauf, K. Do, Pectin methyl esterase from Aspergillus aculeatus : expression cloning in yeast and characterization of the recombinant enzyme, Biosystems. 712 (1996) 705–712.

[34] N.Q. Khanh, E. Ruttkowski, K. Leidinger, H. Albrecht, M. Gottschalk, Characterization and expression of a genomic pectin methyl esterase-encoding gene in Aspergillus niger, Gene. 106 (1991) 71–77. https://doi.org/10.1016/0378-1119(91)90567-U.

[35] D. Bonivento, D. Pontiggia, A. Di Matteo, Fernandez-Recio, G. Juan Salvi, D. Tsernoglou, F. Cervone, G. De Lorenzo, L. Federici4, Crystal structure of the endopolygalacturonase from the phytopathogenic fungus Colletotrichum lupini and its interaction with polygalacturonase-inhibiting proteins, Proteins. 70 (2008) 311–319. https://doi.org/10.1002/prot.

[36] K. Johansson, M. El-Ahmad, R. Friemann, H. Jörnvall, O. Markovič, H. Eklund, Crystal structure of plant pectin methylesterase, FEBS Lett. 514 (2002) 243–249. https://doi.org/10.1016/S0014-5793(02)02372-4.

[37] O. Markovič, H. Jörnvall, Disulfide bridges in tomato pectinesterase: Variations from pectinesterases of other species; conservation of possible active site segments, Protein Sci. 1 (1992) 1288–1292. https://doi.org/10.1002/pro.5560011007.

[38] L.M. Kent, T.S. Loo, L.D. Melton, D. Mercadante, M.A.K. Williams, G.B. Jameson, Structure and properties of a non-processive, salt-requiring, and acidophilic pectin methylesterase from aspergillus Niger provide insights into the key determinants of processivity control, J. Biol. Chem. 291 (2016) 1289–1306. https://doi.org/10.1074/jbc.M115.673152.

[39] S.W. Cho, S. Lee, W. Shin, The X-ray structure of Aspergillus aculeatus Polygalacturonase and a Modeled structure of the Polygalacturonase-Octagalacturonate Complex, J. Mol. Biol. 311 (2001) 863–878. https://doi.org/10.1006/jmbi.2001.4919.

[40] O. Markovič, Š. Janeček, Pectin degrading glycoside hydrolases of family 28: sequence-structural features, specificities and evolution, Protein Eng. Des. Sel. 14 (2001) 615–631. https://doi.org/10.1093/protein/14.9.615.

[41] K.-C. Park, S.-J. Kwon, P.-H. Kim, T. Bureau, N.-S. Kim, Gene structure dynamics and divergence of the polygalacturonase gene family of plants and fungus., Genome. 51 (2008) 30–40. https://doi.org/10.1139/G07-093.

[42] G. Van Pouderoyen, H.J. Snijder, J.A.E. Benen, B.W. Dijkstra, Structural insights into the processivity of endopolygalacturonase I from Aspergillus niger, FEBS Lett. 554 (2003) 462–466. https://doi.org/10.1016/S0014-5793(03)01221-3.

[43] R.P. Jolie, T. Duvetter, A.M. Van Loey, M.E. Hendrickx, Pectin methylesterase and its proteinaceous inhibitor: A review, Carbohydr. Res. 345 (2010) 2583–2595. https://doi.org/10.1016/j.carres.2010.10.002.

[44] Z. Zhang, J. Dong, D. Zhang, J. Wang, X. Qin, B. Liu, X. Xu, W. Zhang, Y. Zhang, Expression and characterization of a pectin methylesterase from Aspergillus niger ZJ5 and its application in fruit processing, J. Biosci. Bioeng. 126 (2018) 690–696. https://doi.org/10.1016/j.jbiosc.2018.05.022.

[45] C. Remoroza, M. Wagenknecht, H.C. Buchholt, B.M. Moerschbacher, H. Gruppen, H.A. Schols, Mode of action of Bacillus licheniformis pectin methylesterase on highly methylesterified and acetylated pectins, Carbohydr. Polym. 115 (2015) 540–550. https://doi.org/10.1016/j.carbpol.2014.09.016.

[46] E. Dheilly, S. Le Gall, M.C. Guillou, J.P. Renou, E. Bonnin, M. Orsel, M. Lahaye, Cell wall dynamics during apple development and storage involves hemicellulose modifications and related expressed genes, BMC Plant Biol. 16 (2016). https://doi.org/10.1186/s12870-016-0887-0.

[47] J.A. de Vries, F.M. Rombouts, A.G.J. Voragen, W. Pilnik, Comparison of the structural features of apple and citrus pectic substances, Carbohydr. Polym. 4 (1984) 89–101. https://doi.org/10.1016/0144-8617(84)90016-X.

[48] O. Markovič, E. Cederlund, W.J. Griffiths, T. Lipka, H. Jörnvall, Characterization of carrot pectin methylesterase, Cell. Mol. Life Sci. 59 (2002) 513–518. https://doi.org/10.1007/s00018-002-8442-6.

[49] T.M.I.E. Christensen, J.E. Nielsen, J.D. Kreiberg, P. Rasmussen, J.D. Mikkelsen, Pectin methyl esterase from orange fruit : characterization and localization by in-situ hybridization and immunohistochemistry, Planta. 206

(1998) 493–503.

[50] X. Pan, T. Tu, L. Wang, H. Luo, R. Ma, P. Shi, K. Meng, B. Yao, A novel low-temperature-active pectin methylesterase from Penicillium chrysogenum F46 with high efficiency in fruit firming, Food Chem. 162 (2014) 229–234. https://doi.org/10.1016/j.foodchem.2014.04.069.

[51] B.J. Savary, A.T. Hotchkiss, R.G. Cameron, Characterization of a salt-independent pectin methylesterase purified from Valencia orange peel, J. Agric. Food Chem. 50 (2002) 3553–3558. https://doi.org/10.1021/jf020060j.

[52] J.A.E. Benen, H.C.M. Kester, J. Visser, Kinetic characterization of Aspergillus niger N400 endopolygalacturonases I, II and C, Eur. J. Biochem. 259 (1999) 577–585. https://doi.org/10.1046/j.1432-1327.1999.00080.x.

[53] Z. Cheng, D. Chen, Q. Wang, L. Xian, B. Lu, Y. Wei, H. Tang, Z. Lu, Q. Zhu, Y. Chen, R. Huang, Identification of an acidic endo-polygalacturonase from Penicillium oxalicum CZ1028 and its broad use in major tropical and subtropical fruit juices production, J. Biosci. Bioeng. 123 (2017) 665–672. https://doi.org/10.1016/j.jbiosc.2017.01.013.

[54] I. Kars, G.H. Krooshof, L. Wagemakers, R. Joosten, J.A.E. Benen, J.A.L. Van Kan, Necrotizing activity of five Botrytis cinerea endopolygalacturonases produced in Pichia pastoris, Plant J. 43 (2005) 213–225. https://doi.org/10.1111/j.1365-313X.2005.02436.x.

[55] H. Tan, G. Yang, W. Chen, Q. Liu, K. Li, H. Yin, Identification and characterization of thermostable endo- polygalacturonase II B from Aspergillus luchuensis, J. Food Biochem. e13133 (2020) 1–11. https://doi.org/10.1111/jfbc.13133.

[56] A.H. Sassi, H. Tounsi, H. Trigui-Lahiani, R. Bouzouita, Z. Ben Romdhane, A. Gargouri, A low-temperature polygalacturonase from P. occitanis: Characterization and application in juice clarification, Int. J. Biol. Macromol. 91 (2016) 158–164. https://doi.org/10.1016/j.ijbiomac.2016.05.075.

[57] R.I.S. Ladeira Ázar, M. da Luz Morales, G. Piccolo Maitan-Alfenas, D.L. Falkoski, R. Ferreira Alfenas, V.M. Guimarães, Apple juice clarification by a purified polygalacturonase from Calonectria pteridis, Food Bioprod. Process. 9

(2019) 238–245. https://doi.org/10.1016/j.fbp.2019.11.013.

[58] J.D.C. Silva, P.R.L. de França, A. Converti, T.S. Porto, Pectin hydrolysis in cashew apple juice by Aspergillus aculeatus URM4953 polygalacturonase covalently-immobilized on calcium alginate beads: A kinetic and thermodynamic study, Int. J. Biol. Macromol. 126 (2019) 820–827. https://doi.org/10.1016/j.ijbiomac.2018.12.236.

[59] S. Carli, L.P. Meleiro, R.J. Ward, Biochemical and kinetic characterization of the recombinant GH28 Stereum purpureum endopolygalacturonase and its biotechnological application, Int. J. Biol. Macromol. 137 (2019) 469–474. https://doi.org/10.1016/j.ijbiomac.2019.06.165.

[60] Y. Tanaka, T. Suzuki, L. Nakamura, M. Nakamura, S. Ebihara, T. Kurokura, M. Iigo, H. Dohra, N. Habu, N. Konno, A GH family 28 endo-polygalacturonase from the brown-rot fungus Fomitopsis palustris: Purification, gene cloning, enzymatic characterization and effects of oxalate, Int. J. Biol. Macromol. 123 (2019) 108–116. https://doi.org/10.1016/j.ijbiomac.2018.11.004.

[61] L. Rexova-Benkova, The Size of the Substrate-Binding Site of an Aspergillus niger Extracellular Endopolygalacturonase, Eur. J. Biochem. 39 (1973) 109–115.

[62] S. Pagès, W.H.M. Heijne, H.C.M. Kester, J. Visser, J.A.E. Benen, Subsite mapping of Aspergillus niger endopolygalacturonase II by site-directed mutagenesis, J. Biol. Chem. 275 (2000) 29348–29353. https://doi.org/10.1074/jbc.M910112199.

[63] H. Lee, J. Rivner, J.L. Urbauer, N. Garti, L. Wicker, De-esterification pattern of Valencia orange pectinmethylesterases and characterization of modified pectins, J. Sci. OfFood Agric. 88 (2008) 2102–2110. https://doi.org/10.1002/jsfa.

[64] S. Mandelc, B. Javornik, The secretome of vascular wilt pathogen Verticillium albo-atrum in simulated xylem fluid, Proteomics. 15 (2015) 787–797. https://doi.org/10.1002/pmic.201400181.

[65] M.C. Ralet, M.J. Crépeau, H.C. Buchholt, J.F. Thibault, Polyelectrolyte behaviour and calcium binding properties of sugar beet pectins differing in their

degrees of methylation and acetylation, Biochem. Eng. J. 16 (2003) 191–201. https://doi.org/10.1016/S1369-703X(03)00037-8.

[66] P. Davidsson, M. Broberg, T. Kariola, N. Sipari, M. Pirhonen, E.T. Palva, Short oligogalacturonides induce pathogen resistance-associated gene expression in Arabidopsis thaliana, BMC Plant Biol. 17 (2017) 1–17. https://doi.org/10.1186/s12870-016-0959-1.

[67] G. Pogorelko, V. Lionetti, O. Fursova, R.M. Sundaram, M. Qi, S.A. Whitham, A.J. Bogdanove, D. Bellincampi, O.A. Zabotina, Arabidopsis and Brachypodium distachyon transgenic plants expressing Aspergillus nidulans acetylesterases have decreased degree of polysaccharide acetylation and increased resistance to pathogens, Plant Physiol. 162 (2013) 9–23. https://doi.org/10.1104/pp.113.214460.

PRIMARY CELL WALL

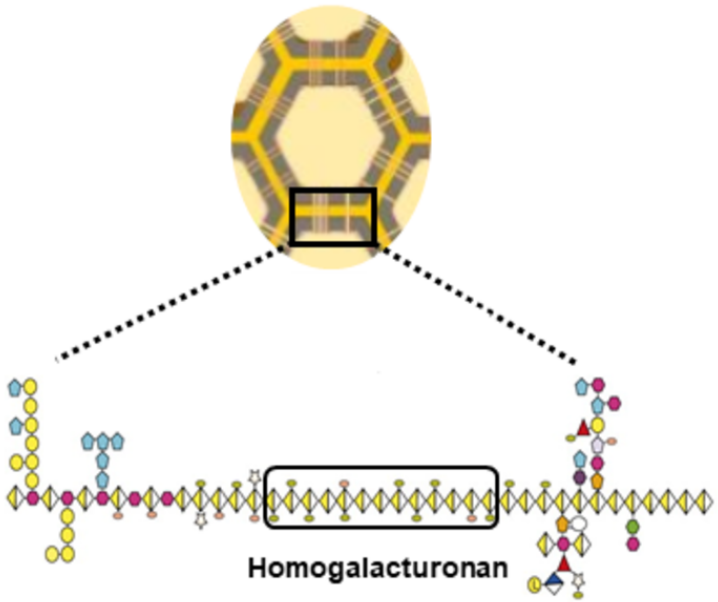

Homogalacturonan degrading enzymes

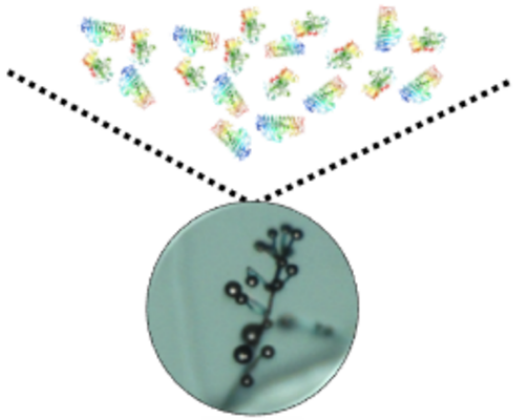

VERTICILLIUM DAHLIAE

HOMOLOGY MODELING

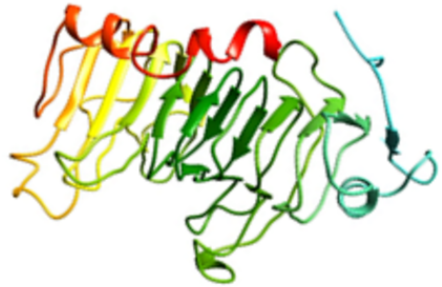

VdPME1

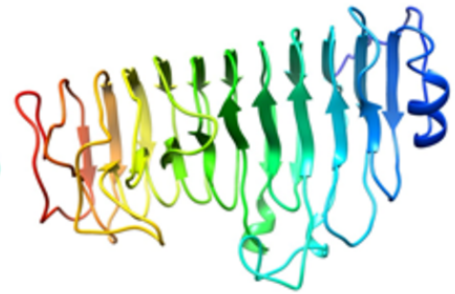

VdPG2

BIOCHEMICAL CHARACTERIZATION

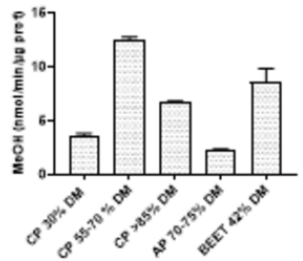

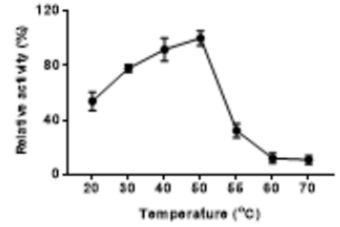

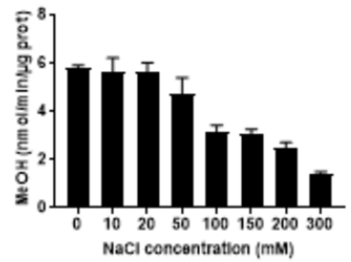

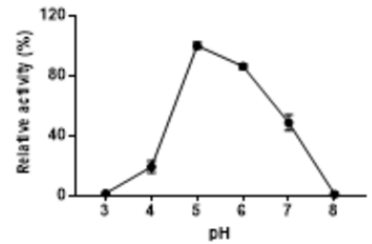

MODE OF ACTION

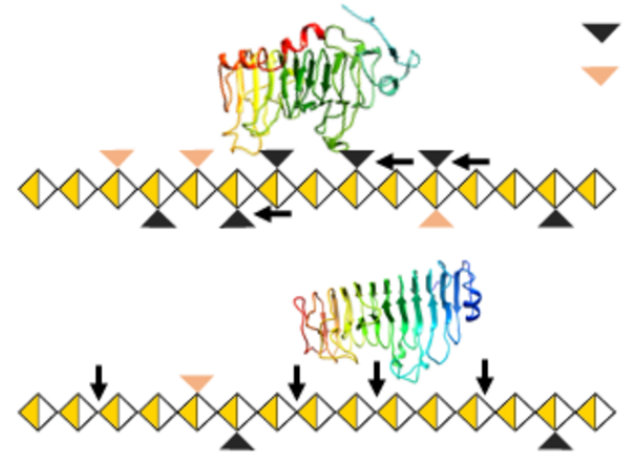

Oligogalacturonides liberated

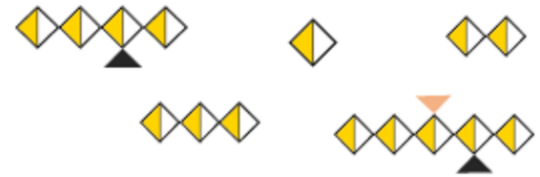

HP-SEC-MS Analysis